JOTCSA
Journal of the Turkish Chemical Society
Section: A
Chemistry

TURKISH
CHEMICAL SOCIETY

# Boronic acid-functionalized silica microparticles for isolation of flavonoids from *Hypericum perforatum*

**Onur Çetinkaya**[1,*], **Hüseyin Çiçek** [2], **Şeyda Kıvrak** [3], G**ülsen Tel Çayan**[4]

[1] *Maria Curie-Sklodowska University, Faculty of Chemistry, 20-031, Lublin/Poland*
[2] *Mugla Sitki Kocman University, Faculty of Science, Department of Chemistry, 48000, Muğla, Turkey*
[3] *Mugla Sitki Kocman University, Faculty of Health Sciences, 48000 Muğla, Turkey*
[4] *Muğla Sıtkı Koçman University, Muğla Vocational School, Department of Chemistry and Chemical Processing Technologies, 48000 Muğla, Turkey*

Abstract: We have selectively separated *cis*- and/or *vicinal*-diol-containing flavonoids from *Hypericum perforatum* (HP) by adsorption/desorption used aminophenylboronic acid (APBA) functionalized uniform (1.6 μm) silica microparticles (BASPs) synthesized *via* the Stöber method. Silica particles were alkylated via its terminal −OH by 3-aminopropyl trimethoxysilane (APTS), glutaraldehyde (GA) and APBA. The results from model adsorption studies were indicated that these microparticles selectively had adsorbed quercetin and rutin but partially apigenin. The antioxidant and antiradical activities of the desorption solution were slightly higher than the post-adsorption solution. These results indicated that the BASP selectively adsorbed the *cis*- and/or *vicinal* antioxidant and antiradical flavonoids.

Keywords: Antioxidants; boronic acids; free radical scavengers; *Hypericum perforatum*; microsphere.

Submitted: April 21, 2017 . Accepted: October 19, 2017.

Cite this: Çetinkaya O, Çiçek H, Kıvrak Ş, Tel Çayan G. Boronic acid-functionalized silica microparticles for isolation of flavonoids from Hypericum perforatum. JOTCSA. 2018;5(1):41–60.

DOI: http://dx.doi.org/10.18596/jotcsa.307440.

* Corresponding author. E-mail: onrctnkya@hotmail.com

## INTRODUCTION

Flavonoids play some important roles in biological and physiological systems of plants (1). They are widely used in health products, cosmetics, and medicines (2-7). Although solvent extraction is the conventional technique (8) to isolate them, this approach leads to environmental pollution due to the large amounts of residual solvents. In addition, these methods are insufficient for the specific isolation of some precious types of flavonoids.

An alternative method for the selective isolation of some types of flavonoids and enrichment of the antioxidant activity of plants involve the uses of adsorbent beads that possess a high surface area and specific functionalities on their surfaces (9-13). In general, the adsorbents used in these studies (*e.g.,* cross-linked polystyrene-based beads) are hydrophobic. The polar/nonpolar ratios can be varied on modification and functionalization of these beads to generate adsorption selectivity to specific types of flavonoids.

Conventionally, uniform micron and submicron silica particles are functionalized with carbon chains, which were selective to some polar/nonpolar groups, have been employed in the columns used in liquid chromatography (14). Hydrophobic interactions and hydrogen bonding can be evaluated as two primary forces to purify or identify the flavonoids. As an alternative packing material or adsorbent, we already reported boronic acid based uniform APBA functionalized poly(chloromethyl styrene-co-divinylbenzene) particles for *cis*- and *vicinal* diol containing flavonoids (15).

Herein we reported silica based microparticles that successfully adsorbed *cis*- and *vicinal* diols (quercetin and rutin as model flavonoids) as compared to the isolated hydroxyl compounds (apigenin). The extraction study was performed on the ethyl acetate extract of *Hypericum perforatum*. As well known, flavonoids possess some antioxidant and antiradical activities. These biological active flavonoids can be selectively separated from the plant extracts. In addition, the prepared uniform microparticles might be useful as the future candidates to be used in liquid chromatography.

## MATERIAL AND METHODS

The tetraethyl orthosilicate (TEOS, 98%, Aldrich, Steinheim, Germany) precursor was used in the synthesis of silica microspheres. *N*-cetyl-*N*,*N*,*N*-trimethylammonium bromide (CTAB, 99%, Merck, Darmstadt, Germany) and dodecylamine (DDA, 98%, Aldrich, Steinheim, Germany) were selected as templating agents. Ethanol (99 %, Sigma-Aldrich, Steinheim, Germany) was used for the

preparation of the dispersion medium. Ammonium hydroxide ($NH_4OH$, 25 %, J.T. Baker, USA) was selected as a catalyst. An aminopropil silane (APTS) (97 %, Aldrich, Steinheim, Germany) and anhydrous toluene (Sigma-Aldrich, USA) were used in the first derivatization step of the silica particles. In the second step, glutaraldehyde (GA, 25 %, Merck, Hohenbrunn, Germany) and aminophenylboronic acid (APBA, 95 %, Aldrich, USA) were used in the boronic acid-functionalization of the particles.

Quercetin hydrate (>95 %, Aldrich, Steinheim, Germany), rutin hydrate (95 %, Sigma, China), and apigenin (95 %, Sigma, USA) were employed as model flavonoids and used in adsorption experiments. Methanol (GC grade, Merck, Darmstadt, Germany), ethanol (Sigma-Aldrich, Steinheim, Germany), and distilled water were used to prepare the adsorption and desorption solutions. 4-(2-Hydroxyethyl)piperazine-1-ethanesulfonic acid (HEPES, 99.5 % Sigma, Steinheim, Germany) was employed to adjust the pH of the solutions. The absorption values of the media were measured with a UV-visible spectrophotometer (Shimadzu W-1601).

Agilent Technologies 1260 Infinity HPLC (high-performance liquid chromatography) (ZORBAX, Eclipse SB-C18, 7 µm, 4.6 mm x 250 mm, Agilent, USA) was used in the chromatography experiments. As a mobile phase, a mixture of methanol–acetonitrile (99.9%, Sigma-Aldrich, France)-ultra distilled water (40:15:45, v/v/v, isocratic) containing 1% acetic acid (100%, Riedel-de Haën, Germany) was selected.

For the free radical scavenging, antioxidant activity, and total flavonoid determination experiments, analytical grade 1,1-diphenyl-2-picrylhydrazyl (DPPH) (85 %, Aldrich, 98 Steinheim, Germany), β-Carotene (97 %, Fluka, USA), Tween-40 (Merck, USA), linoleic acid (99 %, Aldrich, Augsburg, Germany), potassium acetate (>99.0, Merck, Barcelona, Spain), and aluminum nitrate (98.5 %, Merck, Germany) were used. Ethanol and ethyl acetate (99.5 %, Sigma–Aldrich, Steinheim, Germany) were employed as the solvent for the extraction of the plant leaves.

### Synthesis of silica microparticles

The synthesis of BASPs was consisted by four stages, *i.e.* the synthesis of silica microparticles, amine functionalization, activation with glutaraldehyde, and attachment of the APBA ligand. The first stage is the production of silica particles bearing hydroxyl groups on their surface (16), as schematically shown in Fig. 1.

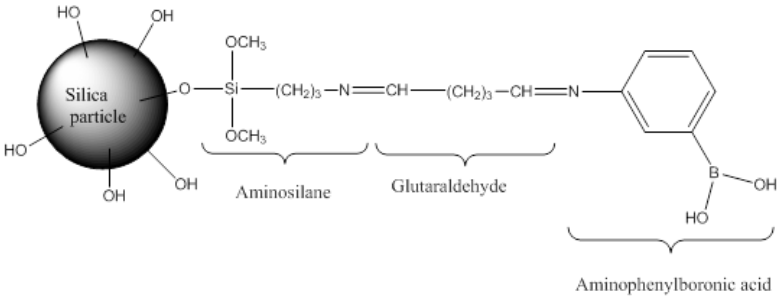


Figure 1: Representation of functionalized silica microparticles.

Silica microparticles were produced using by the conventional sol-gel method at room temperature (17-21). Ethanol (130 mL), distilled water (70 mL), DDA (1.34 g), and CTAB (0.14 g) were mixed in a sealed Pyrex glass bottle until a homogenous solution was obtained. A $NH_4OH$ solution (0.8 mL) was added to solution and immediately stirred. This step was followed by the slow addition of TEOS (5 mL) and the medium was shaken for 2 min. Then, the bottle was firmly closed and stored for 24 h at room temperature. The silica microparticles were washed in two steps to remove surfactants from the interior. First, the silica microparticles were placed in 100 mL of isopropanol and shaken at 70 $^oC$ for 12 h in a shaker (22). Then, the silica microparticles were centrifuged to precipitate and washed again using the same procedure described above. In the last step, the silica microparticles were washed for 30 min under sonication in an ultrasonic ice bath with a concentrated mixture of HCl/ethanol (15/120, v/v) to remove residual surfactants (23). The latter washing process was repeated three times. Silica microparticles bearing hydroxyl functional groups on their surface, which are suitable for derivatization, were obtained.

### Grafting of amine functional group onto the silica microparticles

A small amount of the washed silica microparticles (1.26 g) were dried in an oven at 120 °C. Then, the particles were placed in 10 mL of anhydrous toluene under magnetic stirring (24,25). An excess amount of (3-aminopropyl)triethoxysilane (2 mL), which was dispersed in a tube containing 2 mL of anhydrous toluene, was slowly added to this medium in 10 min under a nitrogen atmosphere and stirred for 2 h to complete the grafting. The particles were centrifuged, placed in 10 mL of anhydrous toluene and washed under stirring. The last washing process was repeated two times. Then, the particles were washed under sonication in an ultrasonic water bath with a HCl/ethanol mixture for 10 min and with distilled water followed by drying in a vacuum oven at 60 $^0C$ for 24 h (26).

### Activation of the amino-capped silica microparticles with glutaraldehyde

The amino-capped silica microparticles were dispersed in a phosphate buffer (0.067 M $KH_2PO_4$ 0.067 M $Na_2HPO_4$) at a pH of 8. Then, 4 mL of GA (25 %) was added dropwise to this solution under stirring (27,28), and the reaction was maintained for 5 h. The silica microparticles became

red that was a sign of successful activation. These particles were washed with distilled water three times.

### APBA attachment to the silica microparticles activated with GA

APBA was attached to the terminal aldehyde on the silica microparticles. For this purpose, 300 mg of APBA was dissolved in 40 mL of distilled water. The pH of this solution was adjusted to 8.0 using 0.1 M NaOH. Approximately 1 g of the amino functionalized silica microparticles was added to the medium under stirring at 200 rpm. The pH of this medium was adjusted to 9.0 with 0.1 M NaOH. The suspension was stirred for 12 h and then centrifuged. The particles were washed for 12 h with a 50 mL of a 1 N NaCl solution, which was adjusted to a pH of 10. Finally, the particles (BASPs) were washed with 0.1 M HCl and distilled water (27). The FT-IR spectra of the particles at each derivatization step were recorded on a Nicolet iS10 FT-IR spectrometer using KBr pellets.

### Model flavonoid adsorption experiments with BASPs

The equilibrium adsorption capacity (Q) (mg flavonoid/g particle) of quercetin, rutin, and apigenin with BASPs were determined in methanol/HEPES buffer (85/25, mL/mL) at 8.5 pH using a UV spectrophotometer per the method of Çetinkaya *et al.* (15). All buffers used for adsorption of model flavonoids, were prepared from methanol/HEPES mixture and specific pH values were adjusted with 0.1 N NaOH.

To show the *cis* and/or *vicinal*-diol selectivity of the adsorbent particles in a mixture, rutin, quercetin and apigenin were used. First, 20 μL solutions of each flavonoid of different concentrations in a methanol/HEPES buffer (pH 8.5) were injected to the HPLC; their retention time versus concentration and calibration curves were determined. Then, the flavonoid mixture in the methanol/HEPES buffer at pH 8.5 was prepared by adjusting the concentration of each flavonoid in the mixture to 25 g/mL. Adsorption was repeated with APBA-attached poly(CMS-co-DVB) particles as described before. The adsorption medium was centrifuged and a supernatant was injected to HPLC. The mobile phase was a mixture of methanol−acetonitrile−water (40:15:45, v/v/v) and 1 % acetic acid as an eluent; column flow rate: 1 mL/min.

### Adsorption experiments with BASPs from HP stem extracts

To investigate the efficiency of BASPs against antiradical and antioxidant activity, ethyl acetate extracts of HP stems (Mugla Turkey) were used in adsorption/desorption experiments. The equation (1) was used to calculate the desorption percent of the adsorbed extract from the adsorbent (29).

$$\%\ Desorption = [Desorbed\ amount\ (mg) / Adsorbed\ amount\ (mg)] \times 100 \quad (1)$$

### Activity measurements using the adsorption solutions

The total flavonoid content (mg flavonoid/g dry weight of extract) of the ethylacetate, adsorption and desorption media were determined separately as described by Moreno *et al.* (30).

Free radical scavenging (DPPH) and *β*-carotene-linoleic acid assay were used to determine the activities of the ethyl acetate extract and adsorption solutions (Ads). In the DPPH method, the free radical scavenging activity was calculated using Equation 2 (31),

$$DPPH\ Scavenging\ Effect\ (\%) = (A_0\text{-}A_1/A_1)\ 100 \qquad \text{(Eq. 2)}$$

where $A_0$ and $A_1$ are the absorbences of the control and sample solutions, respectively. The antioxidant activity was determined using the β-carotene-linoleic acid assay was performed according to the literature method (32).

## RESULTS AND DISCUSSIONS

### Characterization of silica microparticles

The diameters of the synthesized silica microparticles were found between 1.5-1.7 μm by Scanning Electron Microscope (SEM) (JEOL JSM-7600F) (Fig. 2). The pore volume, average pore diameter, specific surface area and external surface area of the silica microparticles were measured by Brunauer–Emmett–Teller (BET) analysis being 0.288 $cm^3/g$, 14 Å, 560 $m^2/g$, and 14.61 $m^2/g$, respectively. According to IUPAC, the physical adsorption isotherm of the particles could be represented as a *Type I* isotherm (33).

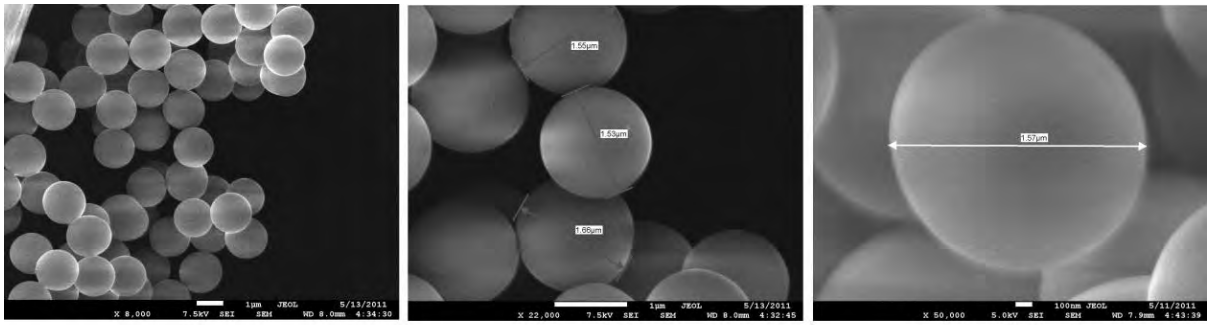


Figure 2: SEM photographs of synthesized silica microparticles (magnifications a: 8,000x; b: 22,000x, c: 50,000x).

The prepared BASPs had a smaller pore volume and the pore size compared to poly(7-oxonorbornene-5,6-dicarboxylic acid-block-norbornene) [poly-(ONDCA-b-NBE)]-coated silica particles that had a 50 Å pore size, 7 μm diameter, 0.8 $cm^3/g$ pore volume and 420 $m^2/g$ surface

area (34). The very small pore volume and porosity properties of BASPs had a disadvantage in adsorption experiments due to their less inner surface area. However, the surface properties, monodispersity and sub-micron particle size of BASPs made it suitable for use in liquid chromatography for the fast determination of flavonoids in plant extracts (34) and could be an alternative to octadecyl-type silica particles (14). Pore size enlargement, which could be achieved by post-synthetic hydrothermal treatment under specific conditions or using by oligomeric and polymeric templates (20), was not applied in this study.

FT-IR analysis of the APBA-functionalized silica microparticles

The silica microparticles were derivatized via the hydroxyl groups on their surface. The first step was involved the covalent attachment of the methoxy group of the silane compound (APTS) via condensation with hydroxyl groups on the surface of the silica particles. The FTIR spectra of synthesized silica microparticles itself (a), washed with HCl/Ethanol (b), modified with APTS (c) and modified with APBA (d) are given in Figure 3.

The band located at 3500 $cm^{-1}$ corresponds to the Si-OH vibration as seen in Figure 3(a). The band between 1950 $cm^{-1}$ and 1850 $cm^{-1}$ can be attributed to the Si-O-Si vibration (27, 35). Another band at 1640 $cm^{-1}$ is most likely due to the OH bending vibration. The two bands located at 2850-2950 $cm^{-1}$ correspond to the symmetric and asymmetric stretching vibrations of $CH_2$ and $CH_3$; present in the CTAB and DDA structures. After the microparticles were washed with HCl and ethanol mixture, these bands nearly disappeared (Figure 3(b)).

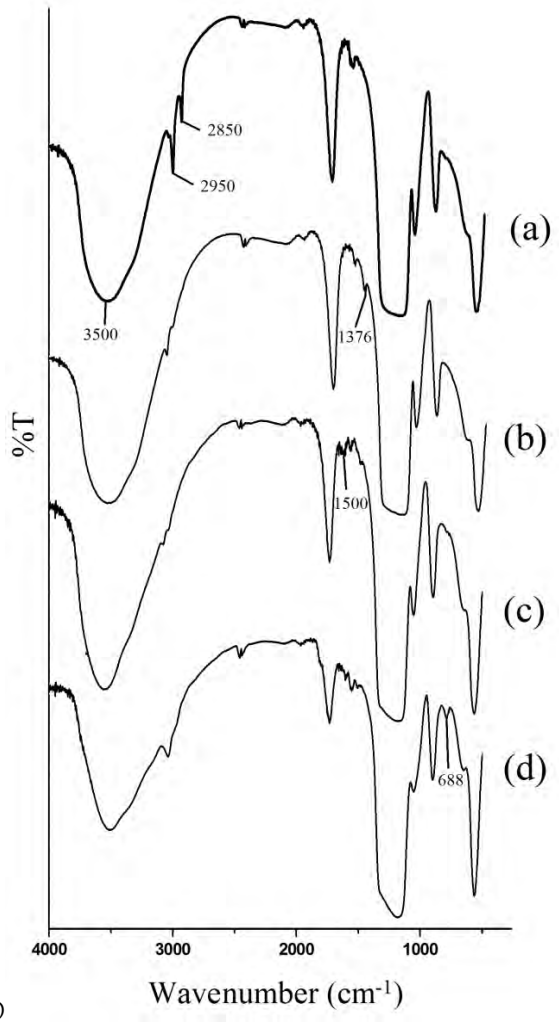


@

Figure. 3: FT-IR spectra of silica microparticles at different functionalization stages; (a) after synthesis, (b) after washed with HCl/ethanol (c) modified with APTS (d) modified with APBA.

In Figure 3 (c), the disappearance of the band located at 1376 $cm^{-1}$ corresponds to the missing Si-OH. The band at 1500 $cm^{-1}$ was due to the secondary amine of APTS (36). The GA attachment is determined by the change in color of the particles due to the shift reaction occurring between the APTS functionalized silica particles and GA. Due to GA and APBA attachment to the surface of the silica particles, the intensity of symmetric and asymmetric stretching vibration bands of the $CH_2$ and $CH_3$ peaks at approximately 2940 $cm^{-1}$ were increased and peak between 3000-3500 $cm^{-1}$ came to fruition (Figure 3 (d)). In addition, the peak that appeared at 688 $cm^{-1}$ (Figure 3d), which was not observed in Figure 3 (c) due to the aromatic structure of APBA.

## Model flavonoid adsorption with BASPs

The selectivity of BASPs for the *cis* and *vicinal*-diol (rutin) and *vicinal*-only-diol-containing model flavonoids (quercetin) were studied. Apigenin was selected as a model flavonoid that does not contain either *cis*- or *vicinal*-diol. The maximum solubility of quercetin was calculated as 0.02

mg/mL. To compare each flavonoid, this value was employed to investigate the effect of the pH on the adsorption capacity.

At a pH of about 8.5, the geometry of BASPs converts from trigonal to a tetrahedral (37). The tetrahedral formation is the most suitable form to capture *cis*- and/or *vicinal*-diols. Therefore, the adsorption capacity of quercetin was higher at a pH 8.5 compare to the pH values (Fig. 4).

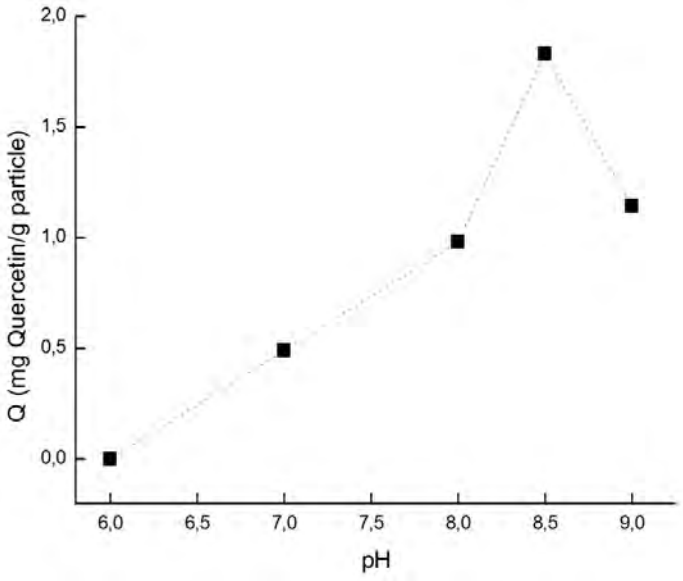


Figure 4: Quercetin adsorption capacity of BASPs at different pHs, temperature: 20 °C, initial quercetin concentration: 0.02 mg/mL.

The variation in the maximum adsorption capacity as a function of pH using BASPs for quercetin, rutin, and apigenin were also comparatively studied. The adsorption capacity at a pH 8.5 of apigenin, which does not contain *cis*- either *vicinal*-diol group, was less than that of rutin and quercetin (Figure 5). At this pH, the adsorption capacity of quercetin and rutin was 2 and 3 mg/g particle, respectively.

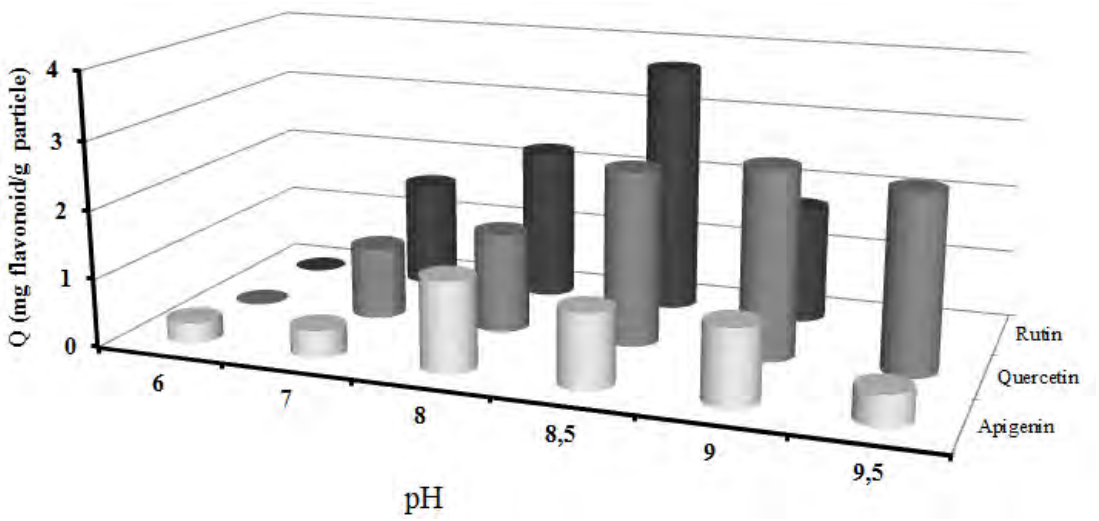


Figure 5: Adsorption capacities of BASPs against quercetin, rutin and apigenin at different pHs; temperature: 20 °C, initial flavonoid concentration: 0.02 mg/mL.

The molecular weight of rutin is twice than that of quercetin. In this study, g/mL of the samples were used instead of moles/mL. From that point of view, the rutin concentration (in moles) becomes half of that for quercetin. As Figure 6 shows, almost similar amount of Desp (rutin and quercetin) were obtained by BASPs. As a whole, the amount of rutin adsorbed on the BASPs become twice as that of quercetin. It may be explained by the fact that the binding probability of quercetin carrying one *vicinal*-diol group to bond to the boronic acid of BASPs is same with rutin carrying *cis*- as well as *vicinal*-diols.

The steric effect of rutin might negatively affect its adsorption on the adsorbent. However, the adsorption capacity of apigenin, which did not contain *cis*-diol groups, did not increase with pH and was less than that of *cis*- and *vicinal*-diol-containing rutin and *vicinal*-diol containing quercetin in the alkaline pH region. However, its amount of adsorption capacity was not rendered negligible which could be attributed to the nonspecific adsorption of apigenin on the adsorbent particles. The nitrogen on the spacer arm (Fig. 1) attached to the silica particles can make a hydrogen bond via the -OH located on the apigenin. Therefore, a comparable amount of apigenin can be isolated with BASPs particles, and this amount does not depend on pH.

The maximum adsorption capacity for quercetin was found as approx. 22 mg/g particle (Figure 6 and Table 1). The compatibility of quercetin adsorption with two well-known adsorption models *i.e.* Langmuir and Freundlich (29,37) was also tested. The $q_o$ values obtained from the Langmuir and Freundlich models were found as 15.43 mg/g and 22 mg/g, respectively, very close to each other. The "K" and "$R^2$" values, which are the equilibrium constant and the coefficient of determination, respectively, were calculated as 17.05 and 0.9755, respectively. $R^2$ obtained from Langmuir model

is sufficiently high as compared to the Freundlich model *i.e.* 0.8515. Therefore, the quercetin adsorption process can be adequately represented by the Langmuir model. However, the model parameters calculated for the Freundlich model were not acceptably suitable for representing this process.

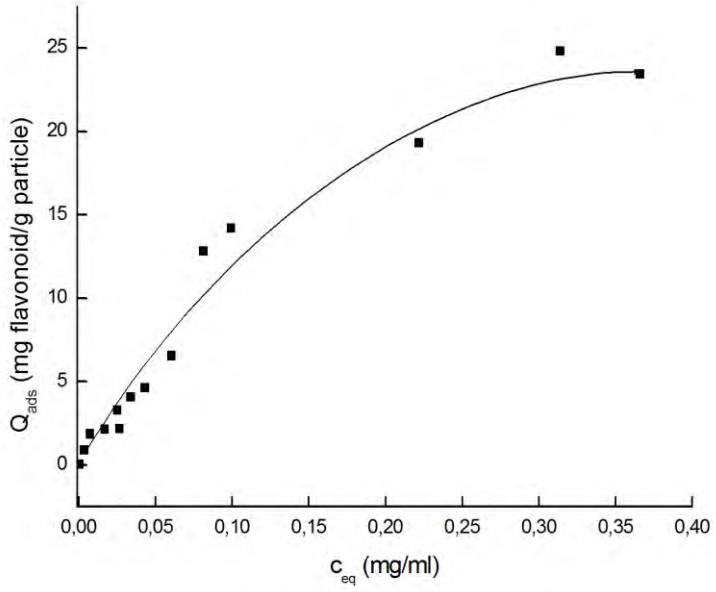


Figure 6: The variation of equilibrium quercetin concentration with initial quercetin concentration for BASPs, temperature: 20 °C, initial flavonoid concentration: 0.02 mg/ml, pH: 8.5.

Table 1 Langmuir and Freundlich model parameters calculated for adsorption of quercetin by using the data obtained from Fig. 6

| Langmuir | | | Freundlich | | |
|---|---|---|---|---|---|
| $q_o$ (mg/g) | $K$ (mg/ml) | $R^2$ | $n$ | $k$ | $R^2$ |
| 15.43 | 17.05 | 0.9755 | 0.6701 | 0.4217 | 0.8515 |

Adsorption selectivity of BASPs towards a model flavonoid mixture

The selectivity of the APBA-attached microparticles to the *cis*- and/or *vicinal*-diols (*i.e.,* quercetin and rutin) is shown in Fig. 7. 2 g of quercetin and 1.9 g of rutin were adsorbed per gram of BASPs. Amounts were obtained from the area under the peaks from HPLC chromatogram. As boronic acid is prone to *cis*- and/or *vicinal*-diols, out of the mixture, the adsorption capacity of apigenin was far more less than the sole apigenin solution. BASPs mostly adsorbed the quercetin and rutin. We can say that, the BASPs selectively adsorbed the flavonoids that contained *cis*- and/or *vicinal*-diols.

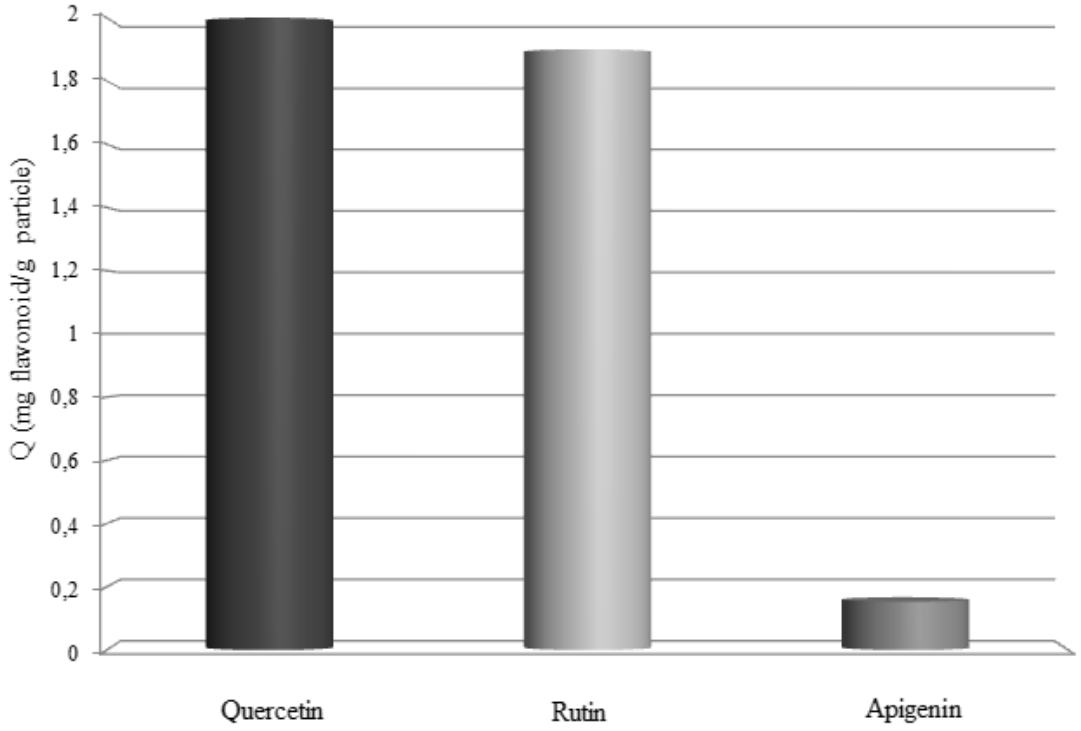


Figure 7: Amount of desorbed flavonoids (quercetin, rutin and apigenin) from BASPs after the adsorption, temperature: 20 ºC, initial flavonoid concentration: 0.02 mg/mL, pH: 8.5.

*Adsorption selectivity of BASPs towards ethyl acetate extract of the HP stem*

The adsorption of flavonoids from the ethyl acetate extract of the HP was compared to the HPLC peaks of the original extract as well as the unadsorbed and desorbed solutions. Fig. 8A shows various peaks *i.e.* original ethyl acetate extract (EtOAc), extract after adsorption (Ads), solution after desorption (Desp) and standards (quercetin and rutin). Ethyl acetate extract shows lots of peaks around 27-31 retention time in the chromatogram. The Desp chromatogram also contains peaks at that area. Probably they are peaks related to *vicinal*-diols containing flavonoids, or *cis*-diol sugars. BASPs has selectivity towards the stated diols, but this selectivity is unaffected by the molecular weight of the compounds. the zoomed area of the chromatogram (Fig. 8B) shows the presence of rutin and quercetin in the extract (EtOAc) that was successfully adsorbed by BASPs (Ads) and then desorbed (Desp). However, slight amount of rutin remained in the post-adsorption medium; probably due to the steric effect of rutin.

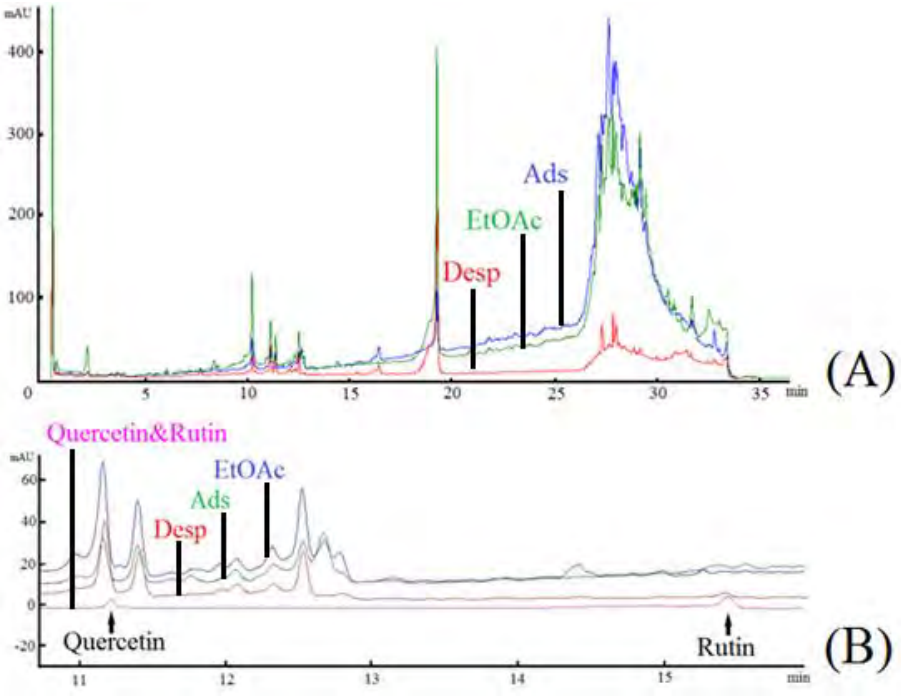


Figure 8: The HPLC chromatogram of original ethyl acetate extract of HP stems; (A) Retention time: 0-35 min, (B): Retention time: 10-16 min of (A) with Quercetin and Rutin model flavonoids.

The dry weight of the original ethyl acetate extract (EtOAc) solution, after adsorption (Ads) and of the desorbed solution (Desp) were calculated as 57.4 mg, 39.1 mg, and 18.3 mg, respectively. By using these three values in Eq. (1), the desorption yield was calculated as 100%. This result was obtained with BASPs after the 40$^{th}$ use. It means the prepared microparticles are able to be regenerated with no efficiency loss.

The total flavonoid content (mg flavonoid/g dry weight of extract) of the EtOAc, Ads, and Desp media were approximately determined to be 48.54 mg/g, 20.16 mg/g, and 35.89 mg/g, respectively, as shown in Fig. 9. In this figure, the total flavonoid content of the Desp medium is higher than that of the Ads medium, which indicates the selectivity of BASPs towards the flavonoids.

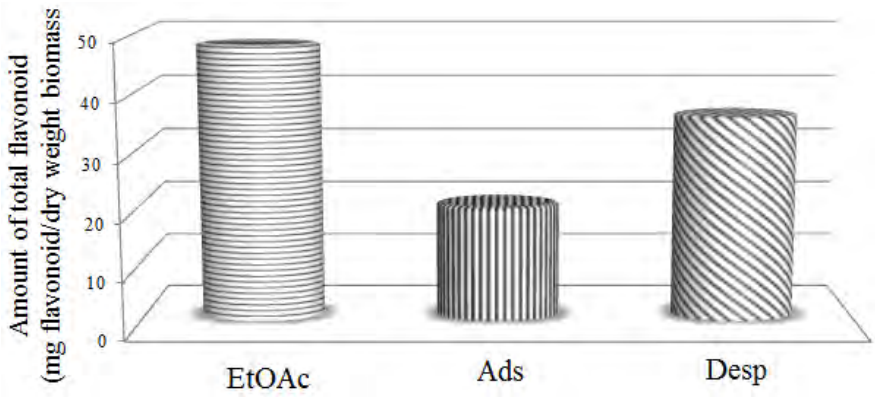


Figure 9: Total flavonoid content of the original solution of ethyl acetate extract of HP stems before adsorption (EtOAc), post-adsorption solution (Ads), and desorption solution (Desp).

Antioxidant and antiradical activities

The antioxidant activity results with the β-carotene and linoleic system for the ethyl acetate extract of the HP stems are shown in Fig. 10 (A). The antioxidant activities of the three media are in the following order: EtOAc > Desp > Ads. These results are parallel to the flavonoid content of the three media, as shown in Figure 9. According to these results, the adsorbed molecules provides slightly better antioxidant activity than the unadsorbed molecules. The amount of flavonoids in the ethyl acetate extract of the HP stems were reported to be high (38,39). In this study, antioxidant activity observed was higher that was also expected.

The rate of β-carotene bleaching of the ethyl acetate extract of the HP stems and its adsorption/desorption solutions are shown in Fig. 10 (B). An interesting result was observed in Fig. 10 (B) where the desorption solution exhibited a higher antioxidant activity rate than the ethyl acetate and post-adsorption (Desp) solutions.

According to the literature (40,41), flavonoid aglycones (*i.e.,* quercetin, kaempferol and biapigenin) have higher antioxidant activities as compared to other flavonoids. In contrast, the antiradical scavenging properties of glycoside-containing flavonols *i.e.,* rutin, hyperoside, isoquercitrin, and kaempferol were determined as higher than the other components. The base structure of BASP exhibits a hydrophilic character, but their surface is covered with space arms containing polar (amide groups and boronic acid tip) and apolar "$CH_2$" molecules due to APTS/APBA and glutaraldehyde molecules, respectively. A suitable apolar/polar ratio in the adsorbent causes a shift in the adsorption of flavonoids from plant extracts (12). While the increment in this ratio causes an increment in the nonspecific adsorption, its decrease results in a smaller adsorption capacity for flavonoids.

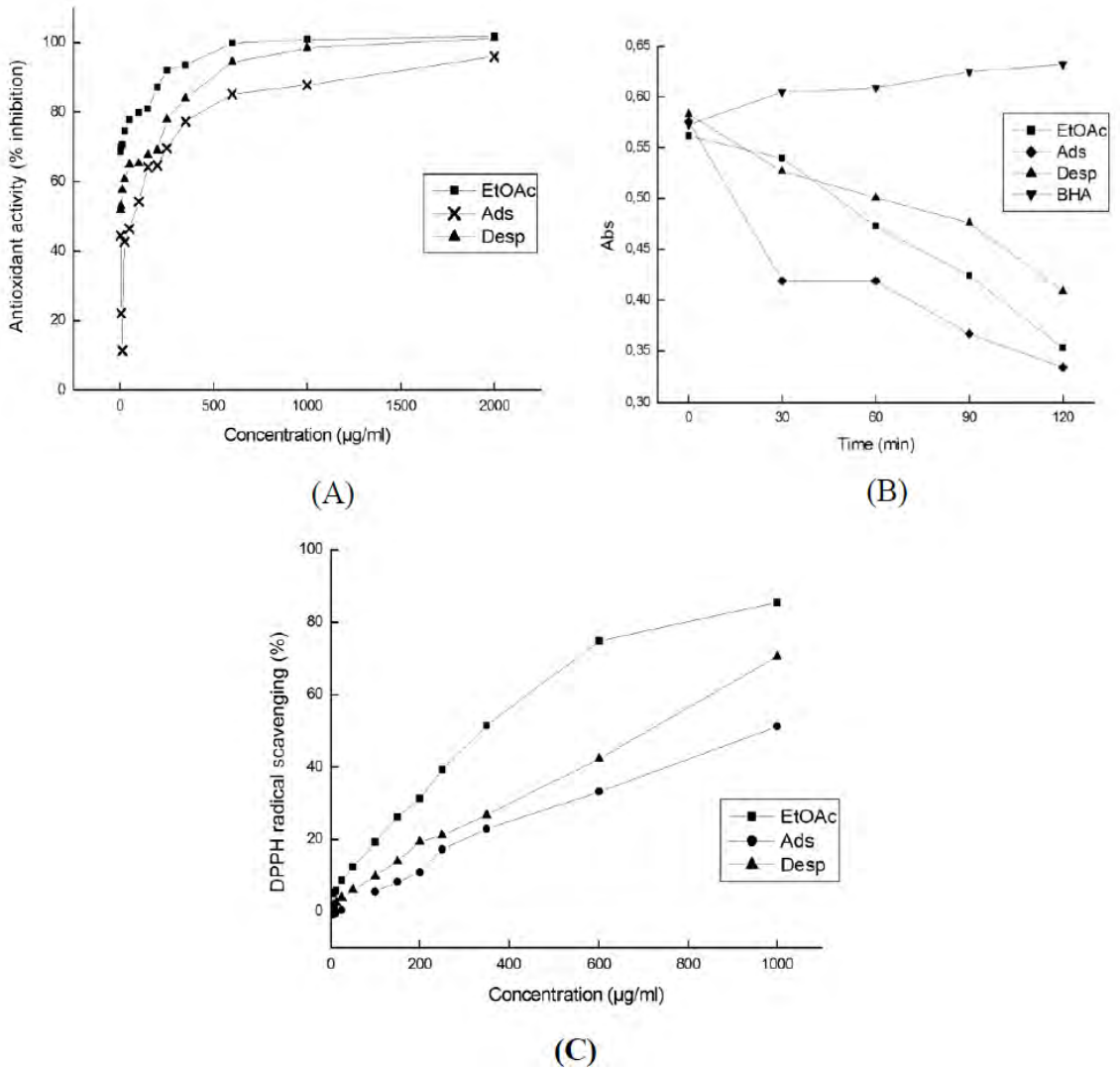


Figure 10: Antioxidant activity (A), rate of β-carotene bleaching (BHA: Butylated hydroxyanisole) (B) and DPPH radical scavenging (C) of the original extract solution of the ethyl acetate extract of the HP stems before adsorption (EtOAc), post-adsorption solution (Ads), and desorption solution (Desp).

Considering these observations, the behavior in Fig. 10 (B) can be clarified by adsorption of more apolar flavonoid aglycones bearing antioxidants rather than polar flavonol glycosides. It is likely that a suitable apolar/polar ratio in BASPs might cause quercetin-type flavonoid aglycones moving close to the spacing arm (Fig. 1) to generate a hydrophobic interaction with the hydrophobic sides of the connecting arm and boronic acid affinity interaction with the *cis*-and/or *vicinal*-diols on the boronic acid side groups while simultaneously applying slightly repulsive forces to flavonol glycoside-type molecules. However, there is a possibility for hydrogen bonding interactions between polar flavonol glycosides and the amine groups on spacing arm. Boronic acids prefer to bind *cis*-and/or *vicinal* diols. That is why, it interacted more with the rutin and quercetin as compared to the apigenin. As discussed in our previous study, flavonoid aglycones isolated by BASPs exhibit a high antioxidant capability (15). Therefore, isolated fractions containing more *cis*-

diol-containing flavonoid molecules exhibited high initial antioxidant velocity, as shown in Fig. 10 (B).

For DPPH radical scavenging (Fig. 10C), the trend in the radical scavenging capacity was approximately the same as that for the antioxidant activity shown in Fig. 10 (A). To compare DPPH activities, $EC_{50}$ (effective concentration for 50 % percent activity) values were calculated for EtOAc, Ads, and Desp as 350, 1000 and 730 (µg dwb/mL), respectively.

These results demonstrate that the DPPH activity of the Desp medium was higher than that of the Ads medium, which may be due to the greater adsorption of flavonoids possessing high antioxidant activity and DPPH radical scavenging properties (40).

## CONCLUSIONS

The APBA-functionalized silica particles (BASPs) synthesized in this study exhibited selectivity towards *cis* ($sp^3$ carbons) as well as *vicinal* ($sp^2$ carbons) diols containing flavonoids. *Cis*-diol-containing flavonoids might be partially isolated with this new adsorbent. However, the presence of other polar/apolar groups present on the silica macroparticles may cause a decrease in the selectivity of the boronic acid groups. Therefore, the DPPH radical scavenging capacity and antioxidant activity of the desorption solution were determined to be lower than that of the original ethyl acetate extract but higher than the post-desorption (Desp) solution. A desorption yield of 100 % for BASPs demonstrates its for studying adsorption phenomena in plant extracts containing *cis*-diol type flavonoids. Uniform adsorbent particles produced in this research have the potential to be used in HPLC chromatography for effective isolating *cis* and/or *vicinal* diols containing compounds.

## ACKNOWLEDGMENTS

We are grateful to the Scientific Research Projects Office (BAP) of Mugla Sitki Kocman University (Project Number 10/25) for their financial support.

## REFERENCES

1. Rijke E, Out P, Niessen WMA, Ariese F, Gooijer C, Brinkman UAT. Analytical separation and detection methods for flavonoids. J. Chromatogr. A 2006; 1112:31-63.

2. Middleton E, Kandaswami C, Theoharides TC. The effects of plant flavonoids on mammalian cells:

implications for inflammation, heart disease, and cancer. Pharmacol. Rev. 2000; 52:673−751.

3. Havsteen BH. The biochemistry and medical significance of the flavonoids. Pharmacol. Ther. 2002; 96(2-3):67−202.

4. Georgetti SR, Casagrande R, Di Mambro VM, Azzolini AE, Maria J. Evaluation of the antioxidant activity of different flavonoids by the chemiluminescence method. Am. Assoc. Pharm. Sci. J. 2003; 5(2):1-4.

5. Walle T. Absorption and metabolism of flavonoids. Free Radic. Biol. Med. 2004;7:829-837.

6. Mak P, Leung YK, Tang WY, Harwood C, Ho SM. Apigenin suppresses cancer cell growth through ERB 1. Neoplasia 20068(11):896−904.

7. Bayard V, Chamorro F, Motta J, Hollenberg NK. Does flavanol intake influence mortality from nitric oxide-dependent processes? Ischemic heart disease, stroke, diabetes mellitus, and cancer in Panama. Int. J. Med. Sci. 2007;4(1):53−58.

8. He DH, Otsuka H, Hirata E, Shinzato T, Bando M, Takeda Y. Tricalysiosides A-G: rearranged ent-kauranoid glycosides from the leaves of tricalysia Dubia. J. Nat. Prod. 2002;65:685−688.

9. Aehle E, Grandic SR, Ralainirina R, Rosset SB, Mesnard F, Prouillet C, Maziere JC, Fliniaux MA. Development and evaluation of an enriched natural antioxidant preparation obtained from aqueous spinach (spinacia oleracea) extracts by an adsorption procedure. Food Chem. 2004;86:579-585.

10. Huang J, Liu Y, Wang X. Selective adsorption of tannin from flavonoids by organically modified attapulgite clay. J. Hazard Mater. 2008;160:382−387.

11. Singh SV, Gupta AK, Jain RK. Adsorption of naringin on nonionic (neutral) macroporus adsorbent resin from its aqueous solutions. J. Food Eng. 2008;86:259−271.

12. Geng X, Ren P, Pi G, Shi R, Yuan Z, Wang C. High selective purification of flavonoids from natural plants based on polymeric adsorbent with hydrogen-bonding interaction. J. Chromatogr. A 2009;1216:8331−8338.

13. Li J, Chase HA. Characterization and evaluation of a macroporous adsorbent for possible use in the expanded bed adsorption of flavonoids from ginkgo biloba l. J. Chromatogr. A 2009;1216:8730−8740.

14. Spacil Z, Novakova L, Solich P. Analysis of phenolic compounds by high performance liquid chromatography and ultra performance liquid chromatography. Talanta 2008;76:189−199.

15. Çetinkaya O, Duru ME, Çiçek H. Synthese and characterization of boronic acid functionalized macroporous uniform poly (4-chloromethylstyrene-co-divinylbenzene) particles and its use in the isolation of antioxidant compounds from plant extracts. J. Chromatogr. B 2012;909:51− 60.

16. Kamiya H, Mitsui M, Takano H, Miyazawa S. Influence of particle diameter on surface silanol structure, hydration forces, and aggregation behavior of alkoxide-derived silica particles. J. Am. Ceram. Soc. 2000;83(2):287−293.

17. Grün M, Lauer I, Unger KK. The Synthesis of micrometer- and submicrometer-size spheres of ordered mesoporous oxide MCM-41. Adv. Mater. 1997;9:254−257.

18. Kresge CT, Leonowicz ME, Roth WJ, Vartuli JC, Beck JS. Ordered mesoporous molecular sieves synthesized by a liquid-crystal template mechanism. Nature. 1992;359:710−712.

19. Qi L, Ma J, Cheng H, Zhao Z. Micrometer-sized mesoporous silica spheres grown under static conditions. Chem. Mater. 1998;10:1623−1626.

20. Stöber W, Fink A, Bohn E. Controlled growth of monodisperse silica spheres in the micron size range. J. Colloid. Interface Sci. 1968;26:62−68.

21. Unger KK, Kumar D, Grün M, Büchel G, Lüdtke S, Adam T, Schumacher, K, Renker S. Synthesis of spherical porous silicas in the micron and submicron size range: challenges and opportunities for miniaturized high-resolution chromatographic and electrokinetic separations. J. Chromatogr. A 2000;892:47−55.

22. Büchel G, Grün M, Unger KK, Matsumoto A, Kazuo T. Tailored syntheses of nanostructured silicas: control of particle morphology particle size and pore size. Supramolecular Science 1998;5(7):253-259.

23. Möller K, Kobler J, Bein T. Colloidal suspensions of nanometer-sized mesoporous silica. Adv. Funct. Mater. 2007;17:605-612.

24. Guerrero VV, Shantz DF. Amine-functionalized ordered mesoporous silica transesterification catalysts. Ind. Eng. Chem. Res. 2009;48:10375−10380.

25. Ramkumar A, Lal R. Silica nanoparticle tags for capacitive affinity sensors. Conf. Proc. IEEE Eng. Med. Biol. Soc. 2005;1:266-269.

26. Kecht J, Bein T. Microporous and mesoporous materials oxidative removal of template molecules and organic functionalities in mesoporous silica nanoparticles by H2O2 treatment. Microporous Mesoporous Mater. 2008;116:123−130.

27. Koopal LK, Yang Y, Minnaard AJ, Theunissen PLM, Riemsdijk WHV. Chemical immobilisation of humic acid on silica. Colloid. Surf. A 1998;141:385−395.

28. Park SW, Lee J, Hong SI, Kim SW. Enhancement of stability of GL-7-ACA acylase immobilized on silica gel modified by epoxide silanization. Process. Biochem. 2003;39:359-366.

29. Senel S. Boronic acid carrying (2-hydroxyethylmethacrylate)-based membranes for isolation of RNA. Colloid. Surf. A 2003;219:17-23.

30. Moreno MIN, Isla MI, Sampietro AR, Vattuone MA. Comparison of the free radical-scavenging activity of propolis from several regions of Argentina J. Ethnopharmacol. 2000;71(1−2):109−114.

31. Blois MS. Antioxidant determinations by the use of a stable free radical. Nature 1958;26:1199−1200.

32. İlhami G, Oktay M, Kireçci E, Küfrevioglu Öİ. Screening of antioxidant and antimicrobial activities of anise (pimpinella anisum L.) seed extracts. Food Chem. 2003;83:371-382.

33. Sing KSW, Everett DH, Haul RAW, Moscou L, Pierotti RA, Rouquerol J, Siemieniewska T. Reporting physisorption data for gas/solid systems with special reference to the determination of surface area and porosity. Pure&Appl. 1985;57(4):603-619.

34. Huck CW, Buchmeiser MR, Bonn GK. Fast analysis of flavonoids in plant extracts by liquid chromatography-ultraviolet absorbance detection on poly(carboxylic acid)- coated silica and electrospray ionization tandem mass spectrometric detection. J. Chromatogr. A 2001;943:33−38.

35. Weinstock BA, Yang H, Griffiths PR. Determination of the adsorption rates of aldehydes on bare and aminopropylsilyl-modified silica gels by polynomial fitting of ultra-rapid-scanning FT-IR data. Vib. Spectrosc. 2004;35:145−152.

36. Colthup NB. Spectra-structure correlations in the infra-red region. J. Optical Am. 1950;40:397-400.

37. Çiçek H. Nucleotide isolation by boronic acid functionalized hydrogel beads. J Bioact Compat Polym 2005;20:245-257.

38. Butterweck V, Jurgenliemk G, Nahrstedt A, Winterhoff H. Flavonoids from hypericum perforatum show antidepressant activity in the forced swimming test. Planta Med. 2000;66:3−6.

39. Barnes J, Anderson LA, Phillipson JD. St John's Wort (hypericum perforatum l.): a review of its chemistry, pharmacology and clinical properties. J. Pharm. Pharmacol. 2001;53:583−600.

40. Flausino OA, Zangrossi H, Salgado JV, Viana MB. Effects of acute and chronic treatment with

hypericum perforatum l. (li 160) on different anxiety-related responses in rats. Pharmacol. Biochem. Be. 2002;71:251–257.

41. Silva BA, Ferreres F, Malva JO, Dias ACP. Phytochemical and antioxidant characterization of hypericum perforatum alcoholi c extracts. Food Chem. 2005;90:157–167.